NJC
New Journal of Chemistry
A journal for new directions in chemistry

Accepted Manuscript

This article can be cited before page numbers have been issued, to do this please use: A. S. Mac Cormack, M. V. Busch, M. L. Japas, L. Giovanetti, F. Di Salvo and P. H. H. Di Chenna, *New J. Chem.*, 2020, DOI: 10.1039/D0NJ01440K.

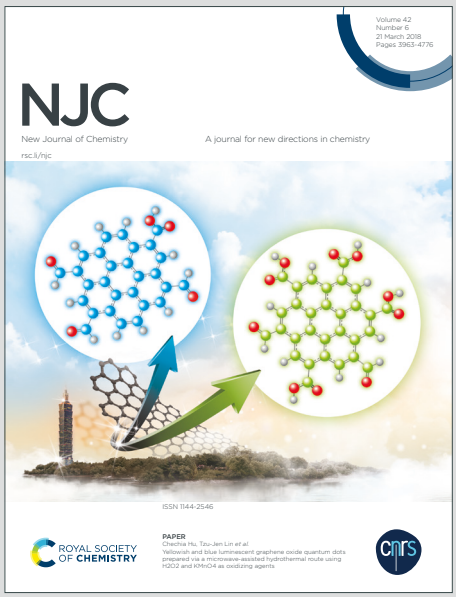

This is an Accepted Manuscript, which has been through the Royal Society of Chemistry peer review process and has been accepted for publication.

Accepted Manuscripts are published online shortly after acceptance, before technical editing, formatting and proof reading. Using this free service, authors can make their results available to the community, in citable form, before we publish the edited article. We will replace this Accepted Manuscript with the edited and formatted Advance Article as soon as it is available.

You can find more information about Accepted Manuscripts in the Information for Authors.

Please note that technical editing may introduce minor changes to the text and/or graphics, which may alter content. The journal's standard Terms & Conditions and the Ethical guidelines still apply. In no event shall the Royal Society of Chemistry be held responsible for any errors or omissions in this Accepted Manuscript or any consequences arising from the use of any information it contains.

View Article Online
DOI: 10.1039/D0NJ01440K

ARTICLE

Effect of vicinal di-halo substituents on the organogelling properties of aromatic supramolecular gelators and their application as soft template

Received 00th January 20xx,
Accepted 00th January 20xx

DOI: 10.1039/x0xx00000x

Andrea S. Mac Cormack,[a] Verónica M. Busch,[b] M. Laura Japas,[c] Lisandro Giovanetti,[d] Florencia Di Salvo[e] and Pablo H. Di Chenna*[a]

A pronounced effect of vicinal dihalogen substituents on the gelling properties of aromatic low molecular weight organogelators is reported. A new family of N,N'-(4,5-dihalogen-1,2-phenylene)dialkylamides with fluorine, chlorine, bromine and iodine was designed and synthesized. A systematic investigation of their organogelling ability, thermic stability, mechanical properties and self-assembled structure was performed to elucidate the effect that the vicinal di-halo substituents have on the organogels. It was found that the presence of two halogen atoms (X) have a determinant effect being the brominated compounds the most general efficient organogelators. In hydrocarbons the gelling ability increased from fluorine to iodine following the halogen bond donor ability trend. SAXS experiments were in agreement with a fibrillar self-assembly where the halogens are located at the surface of the fibers. Multiple cooperative interactions are involved in the self-assembly of the gels: π-π stacking, hydrogen bonds as well as X···X contacts. Thus, this work provides a new strategy for the design of new gelators or to improve the efficiency of known organogelators by introducing two vicinal halogens substituents into aromatic rings. An ethanolic gel was also successfully used as template to prepare silica and titania nanotubes so such organogels are promising materials for future research and development.

Introduction

Molecular gels (also called physical gels) are a special kind of soft materials that originate from the reversible self-assembly of low molecular weight gelators (LMWGs) through non-covalent intermolecular interactions.[1,2] These reversible interactions generate a three dimensional self-assembled fibrillar network (SAFIN) that traps the liquid. Molecular gels are heat responsive materials and the sol-gel transition occurs at a characteristic temperature (T_{gel}) that depends on the gelator, its concentration and the liquid medium.[3] In the last two decades the interest on LMWGs continuously increased due to their unique properties: if the gelator molecule is sensitive to a specific physical or chemical stimuli, the supramolecular gel will respond to the same stimuli and in many cases the sol-gel transition can be triggered by one or more physical (heat, light, sound, etc.)[4] or chemical (pH, ions, redox, etc.) external stimuli.[5] Therefore, supramolecular gels have many potential hi-tech applications *i.e.* in optoelectronic devices,[6,7] chemosensing,[8,9] catalysis,[10] drug delivery,[11,12] bioimaging,[13] pollutant removal,[14] as reaction media,[15–17] self-healing materials,[18] 3D printing,[19] etc. In this context of such interesting applications, modulating the physical, mechanical and chemical properties of molecular gels is a great challenge. Nowadays, even with the knowledge gained on the self-assembly process and the molecular characteristics that lead to the formation of supramolecular gels, it is still not possible to design *de novo* a new molecular gelator and predict its properties.[20,21] Thus, it is crucial to unravel the subtle molecular features that control the self-assembly of LMWGs to be able to design new molecular gels with specific functions and characteristics.

It is known that the assembly of LMWGs can be promoted by multiple non-covalent interactions, being the most usual hydrogen bonding, π-π stacking, van der Waals interactions and solvophobic forces. In the last years the halogen bond[22,23] has been added to the list as a versatile, dynamic, highly directional and tuneable supramolecular interaction that can play a key role in the self-

[a] Universidad de Buenos Aires, Consejo Nacional de Investigaciones Científicas y Técnicas, Unidad de Microanálisis y Métodos Físicos Aplicados a la Química Orgánica (UMYMFOR), Departamento de Química Orgánica, Facultad de Ciencias Exactas y Naturales, Pabellón 2, Ciudad Universitaria, C1428EGA, Buenos Aires, Argentina. *email: dichenna@qo.fcen.uba.ar
[b] Universidad de Buenos Aires, Consejo Nacional de Investigaciones Científicas y Técnicas, Instituto de Tecnología de Alimentos y Procesos Químicos (ITAPROQ) Departamento de Química Orgánica y Departamento de Industrias, Facultad de Ciencias Exactas y Naturales, Ciudad Universitaria, C1428EGA, Buenos Aires, Argentina.
[c] Comisión Nacional de Energía Atómica (CNEA), Gerencia Química, Centro Atómico Constituyentes, Av. Gral. Paz 1499, San Martín, B1650KNA Buenos Aires, and Escuela de Ciencia y Tecnología, Universidad Nacional de San Martín, Martín de Irigoyen 3100, 1650 San Martín, Buenos Aires, Argentina.
[d] Instituto de Investigaciones Fisicoquímicas Teóricas y Aplicadas (INIFTA), Facultad de Ciencias Exactas, Universidad Nacional de la Plata, CONICET, casilla de correo 16, sucursal 4, 1900, La Plata, Argentina.
[e] Universidad de Buenos Aires, Facultad de Ciencias Exactas y Naturales, Departamento de Química Inorgánica, Analítica y Química Física and CONICET, Instituto de Química Física de los Materiales, Medio Ambiente y Energía (INQUIMAE), Buenos Aires C1428EGA, Argentina.

† Electronic Supplementary Information (ESI) available: Synthetic procedures, gel characterization (T_{gel} and CCG), rheology experiments, ^{1}H NMR vs T spectra, SEM images, SAXS and Crystalographyc data. See DOI: 10.1039/x0xx00000x

assembly process of molecular gels.[24,25] The first clear example of a molecular gelation triggered by an halogen bond was reported by Steed *et al.*[26] After this seminal work many other examples of supramolecular gelation with direct evidence of halogen bond control were reported.[27–29] These examples are extreme cases where strong halogen bond interactions were promoted using electron-deficient heavier halogen substituents, such as iodine in perfluorinated aromatic rings, and good halogen bond acceptor atoms such as the basic nitrogen of pyridines. Nevertheless, in recent years it was demonstrated that simple halogen substituents in π-gelators can have a pronounced positive effect on the gelling ability and mechanical properties that can be tuned by varying the halogen.[30–34] These effects have been associated with the fact that halogen substituents can enhance π-π stacking,[31] but also participate in multiple weak interactions such as halogen···π (X···π), C-H···X hydrogen bonding, C-X···O halogen bonding[30,35] and type I and II X···X contacts.[36] Both types of halogen contacts have been widely found in crystalline structures,[37] but in solution and soft materials, like molecular gels, their role has only been studied indirectly.[36] In solid state they are characterized by halogen-halogen distances shorter than the sum of the van der Waals radii. Type II contacts involve the interaction of the electrophilic region of one halogen atom with the nucleophilic region of the other, while type I contacts are likely to minimize repulsion by interfacing neutral regions of their electrostatic potential surfaces. Thus, only type II contacts are considered to be halogen bonds.[38] As can be concluded from these precedents, halogenated organic compounds are of great interest for the rational and systematic design of supramolecular functional materials, in particular molecular gels.

In 1999 Clavier *et al.*[39] reported the gelling ability of a series of simple substituted dialkoxy-benzene compounds. Among them, three 1,2-dibromo-4,5-bis(alkoxy)benzene derivatives with octyl, decyl (**1**) and hexadecyl groups were described as better gelators than the non-brominated analogues concluding that the packing ability of bromine atoms reinforce the strength of the network. Nevertheless, their gelling ability is poor, they can only gel four specific organic solvents at high concentrations (0.05M) and the resultant gels have also a very low thermostability, in fact some of them can only gelate under 0°C (T_{gel}: -15 to 38 °C). Years later, Fonrouge *et al.*[40] reported the crystal structure of one of the gelators, 1,2-dibromo-4,5-bis(decyloxy)benzene (**1**), where type I and II Br···Br contact interactions were observed (Fig. 1). These two independent results allowed us to consider the hypothesis that these Br···Br contacts present in the crystalline network could also be involved in the self-assembly of the molecular gel.

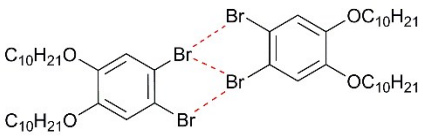

Fig. 1 Representation of type I and II contacts observed in the crystal structure of 1,2-dibromo-4,5-bis(decyloxy)benzene (**1**).

In this context, and continuing with our research on the development of more efficient organogelators[41,42] and the study of their self-assembly,[43,44] we designed a family of vicinal di-halogenated aromatic compounds, with potential organogelling abilities replacing the alkoxy moieties by amide groups, a known strong and highly directional supramolecular synthon that would allow a more stable self-assembly through hydrogen bond, hence better gelators. Here we report the synthesis and systematic study of the halogen effect (F, Cl, Br, I) and alkyl chain length effect on the gelling properties of 20 new N,N'-(4,5-dihalo-1,2-phenylene)dialkylamides analogues (Fig. 2).

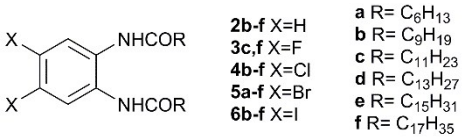

Fig. 2 Chemical structures of the designed N,N'-(4,5-dihalogen-1,2-phenylene)dialkylamides and their non-halogenated analogues.

To the best of our knowledge only one non-halogenated organogelator bearing a 1,2-phenylenedialkylamide moiety has been described and patented as a component of cosmetics and pharmaceutics products.[45] Our design was motivated by the following hypothesis: a) that the presence of two amide groups on the phenyl ring would allow, together with π-π stacking, the one dimensional molecular self-assembly. b) The electronegative character of halogen substituents would enhance the π-π stacking interaction and c) The presence of two vicinal halogen atoms on the phenyl core would improve the gelling property compared to the non-halogenated compounds by complementary and cooperative halogen-halogen contact interactions, already observed for this moiety in solid state.[40,46]

Experimental

Materials and methods

FT-IR spectra of solids were recorded in thin films using KBr discs on a Scientific Nicolet iS50 FT-IR spectrophotometer, values are given in cm^{-1}. ^1H and ^{13}C NMR spectra were recorded on Bruker spectrometers: AVANCE NEO 500 or Fourier 300. Unless specified, NMR experiments were carried out in deuterated chloroform ($CDCl_3$). Chemical shifts (δ) are reported in parts per million (ppm) with reference to tetramethylsilane (TMS) or residual solvent peaks as internal standards. The following abbreviations are used for the proton spectra multiplicities: s: singlet, d: doublet, t: triplet, m: multiplet. High resolution mass spectra (HRMS) were obtained with a Bruker MicroTOF-Q II instrument using electrospray ionization and a time of flight analyzer. When necessary, organic solvents were routinely dried and/or distilled prior to use and stored over molecular sieves under argon. Flash column chromatography was carried out on Merck silica gel S 0.040–0.063 mm. Organic extracts were dried over anhydrous sodium sulfate (Na_2SO_4). 4,5-Dibromobenzene-1,2-diamine was prepared as previously described in literature.[47]

Dynamic rheology. Rheological properties of organogels were evaluated using a controlled shear rheometer (Paar Physica MCR 300, Anton Paar GmbH, Austria) with a 30 mm diameter

View Article Online
DOI: 10.1039/D0NJ01440H

parallel plates geometry and 1 mm of gap between the plates. Triplicates of discs (3 mL, 15 mM of each sample in ethanol) were evaluated. An amplitude sweep was performed with frequency control (1 Hz) in order to establish the viscoelasticity linear range. Dynamic storage modulus (G´) and dynamic loss modulus (G´´) were evaluated by varying the frequency from 0.1 to 100 Hz with a 0.1% strain within the viscoelastic linear ranges. The temperature was controlled at 25.0 ± 0.1 ^{o}C with a Peltier plate. A solvent trap was used and the sample borders were covered with Vaseline in order to protect solvent evaporation. For the sol-gel temperature determination G' was recorded as a function of temperature by heating the sample at a rate of 1 ^{o}C s^{-1}. The rheological sol-gel temperature (Tg) was defined as the point where the G´ was half way between G´ for the solution and G´ for the gel.[48]

Aerogels preparation with supercritical CO_2. Aerogels were prepared from the self-assembled supramolecular gels by drying with supercritical CO_2. The set-up included a high-pressure cylindrical quartz cell (internal volume ca. 4 mL) mounted on a metal frame in a way to allow rocking the cell, a high-pressure syringe (Teledyne ISCO 100DM, capacity 100 mL), high-pressure valves (High Pressure Equipment Co.) and a pressure gauge. The quartz cell was connected, on opposite sides and through high-pressure valves, to the syringe and vent. The quartz cell was placed in a thermostated water bath. Previous to the operation, the syringe was loaded with liquid CO_2 from the tank by circulating cold water (ca 15°C) through its temperature control jacket. A gel sample contained on a cylindrical glass tube (length 2.5 cm, diameter 5 mm) containing 200 μL of organogel was then transferred to the quartz cell and immediately sealed, to avoid solvent evaporation. Liquid CO_2 was then injected into the sample compartment at a flow rate of ca. 100 mL (NPT)·min^{-1}, while the pressure was kept constant at 8 MPa. The temperature of the sample was maintained at ambient value (ca. 20°C) during the solvent-extraction procedure. Once no solvent was visually detected in the cell (absence of refractive index waves while rocking) and in the downstream (no liquid condensation in the collecting tube), the temperature of the sample was raised to 35°C and its pressure slowly reduced, always under supercritical conditions. The drying process took around 3 h.

Scanning electron microscopy (SEM). SEM pictures of the xerogels, aerogels and inorganic nanoparticles were taken on a Carl Zeiss NTS SUPRA 40FEG scanning electron microscope (EHT = 3.00 kV). A small portion of the solid sample was attached to the holder by using a conductive adhesive carbon tape. Prior to examination the xerogels were coated with a thin layer of gold.

Single Crystal X-ray diffraction (XRD) measurements
Single crystals of **5a** and **7** were obtained after slow evaporation of the solvent at RT, using acetone. A suitable crystal for each compound was selected and mounted on a loop and measured with an Oxford Diffraction Gemini Eos diffractometer with Mo Kα (λ = 0.71 Å) radiation and kept at 170 K for **5a** and 293 K for **7** during data collection. The full data collection was planned using CrysAlis Pro strategy tool and data were reduced using CrysAlis Pro programme (Oxford Diffraction/Agilent Technologies UK Ltd, Yarnton, England). A Gaussian method implemented in WinGX[49] or a numerical model was used for the absorption correction. Using Olex2, the structures were solved with the olex2.solve[50] structure solution program using Charge Flipping and refined with the ShelXL[51] refinement package using Least Squares minimization. Non-hydrogen atoms were anisotropically refined and hydrogen atoms were mostly included at geometrically calculated positions with thermal parameters derived from the parent atoms. Hydrogen atoms attached to groups suitable to form hydrogen bonds were first located on Fourier maps, fixed, and the isotropic displacement parameters were given depending on the parent atoms. Idealised methyl group was refined as rotating moiety: C1(H1A,H1B,H1C) for **5a** and C18(H18A,H18B,H18C) for **7**. Structural information is detailed in ESI†. CCDC Deposition Numbers are 1974220 and 1974435 for **5a** and **7**, respectively.

Template polymerization of TEOS. Gelator **5f** (15 mg) was dissolved by heating and shaking in a mixture of ethanol (0.9 mL) and TEOS (0.1 mL) with addition of benzylamine (5 μL) and water (5 μL) as catalysts. The solution was cooled to room temperature until gelation was observed and then left at room temperature for 5 days. Subsequently, the template was dissolved in dichloromethane, the solid was centrifugated, and washed once with dichloromethane. The silica was heated at 200 ^{o}C for 2 h and 600 ^{o}C for 4 h in air.

Template polymerization of Ti(O*i*Pr)$_4$. Gelator **5f** (15 mg) was dissolved in ethanol (0.95 mL) by heating and shaking, then Ti(O*i*Pr)$_4$ (50 μL) was added. The solution was cooled to room temperature until gelation was observed. The flask was left at room temperature semi-closed, in order to allow the moisture to diffuse and slowly initiate the polymerization. After 7 days the template was dissolved in dichloromethane, the solid was centrifugated, and washed once with dichloromethane. The titania was heated at 200 ^{o}C for 2 h and 600 ^{o}C for 4 h in air.

Small angle X-ray scattering (SAXS). SAXS measurements were performed using a XEUSS 1.0 from XENOCS equipment located at the Instituto de Investigaciones Fisicoquímicas Teóricas y Aplicadas (INIFTA-CONICET-UNLP). This setup is equipped with a 2D photon counting pixel X-ray detector Pilatus 100k (DECTRIS, Switzerland). The scattering intensity, I(q), was recorded in the range of the momentum transfer 0.25< q <6.7 nm^{-1}, where $q = 4\pi/\lambda \sin(\theta)$, being 2θ the scattering angle and λ = 0.15419 nm is the weighted average of the X-ray wavelength of the Cu-$K_{\alpha 12}$ emission lines. All measurements were carried out using liquid and gel samples contained in capillary tubes Borokapillaren: outside diameter 1.5 mm, wall thickness 0.01 mm, length 80 mm WJM-Glas/Müller GmbH, Germany. Reported data were corrected for the parasitic scattering and processed using standard procedures. Fitting

View Article Online
DOI: 10.1039/D0NJ01440K

experiments were performed using SasView software version 5.0.0.[52‡]

Results and discussion

Synthesis

The non-halogenated di-amides **2** were prepared by reaction of commercial o-phenylenediamine with the corresponding acid chloride following a standard procedure.[53] Compounds **3**-**6** were synthesized following simple electrophilic aromatic substitution steps, followed by acylation of the corresponding 4,5-dihalogen-1,2-phenylenediamine with acid chlorides. All new compounds were fully characterized (see ESI†). 4,5-Difluoro-1,2-phenylenediamine and 4,5-dichloro-1,2-phenylenediamine were prepared from o-difluorobenzene and o-dichlorobenzene using the methodology described in literature.[54] 4,5-Dibromo-1,2-phenylenediamine was prepared from o-phenylenediamine using the methodology described in literature.[47] 4,5-Diiodo-1,2-phenylenediamine was prepared from commercial o-dinitrobenzene as described in literature.[55]

Gelation ability

The gelling ability of all compounds was tested using the inverted tube method on 34 solvents covering the entire range of polarities, from hydrocarbons to water. The non-halogenated and fluorinated compounds were found to have a similar poor gelling ability. They were insoluble in the majority of the solvents (Table S1, ESI†). The best gelators were compounds **2f** and **3f** bearing the longer alkyl chain (stearylamides) being able to gel only 3 and 4 solvents respectively. The gelling ability improved for the chlorinated analogues **4b-f** (Table 1 and Table S2), gelator **4d** bearing myristylamides was the gelator with the optimal chain length gelling 16 solvents with a wide spectrum of polarities, including a hydrocarbon (*n*-heptane) and polar solvents like ketones and some alcohols. Nevertheless, as for the non-halogenated and fluorinated analogues, the gels were highly opaque probably due to low solubility. The brominated derivatives **5**, direct analogues of the reported gelator **1**,[39,40] were then studied. The compound with the shorter alkyl chain (**5a**) could not gelate any of the tested solvent while the following analogue of the series (**5b**) formed gels with some non-protic polar solvents.

Table 1. Comparative gelation ability and critical concentration for gelation (CCG) of halogenated compounds with F (**3**), Cl (**4**), Br (**5**) and I (**6**) bearing laurylamides (**c**) and myristylamides (**d**) in representative solvents.[a] Complete list can be found at ESI†.

entry	Solvent	3c	4c	5c	6c	4d	5d	6d
1	*n*-Hexane	P	P	P	OG (6.27)	P	P	G (4.91)
2	*n*-Heptane	P	OG (92.5)	OG (22.7)	OG (4.60)	OG (83.6)	OG (9.71)	G (21.3)
3	*n*-Decane	P	P	P	OG (13.8)	P	P	OG (21.3)
4	Cyclohexane	P	P	OG (8.81)	OG (13.8)	P	G (8.09)	OG (10.7)
5	Ethyl ether	P	P	G (6.34)	I	P	G (5.20)	P
6	Isopropyl ether	P	P	G (2.27)	OG (23.0)	P	G (4.85)	P
7	1,2-Dichloroethane	P	OG (30.8)	G (3.60)	G (13.8)	P	G (7.28)	OG (9.15)
8	Dichloromethane	P	P	G (15.6)	G (13.8)	OG (41.8)	G (9.10)	G (4.91)
9	CCl_4	P	P	OG (52.9)	P	P	OG (29.1)	P
10	Chloroform	S	S	S	G (69.0)	P	G (16.2)	G (12.8)
11	Acetonitrile	P	OG (1.85)	G (0.32)	P	OG (41.8)	G (0.29)	P
12	Ethyl acetate	P	P	G (3.30)	G (13.8)	P	G (4.85)	G (5.43)
13	Ethanol	P	OG (18.5)	G (3.17)	G (5.75)	G (20.9)	G (4.41)	OG (8.01)
14	Isopropanol	P	OG (46.3)	G (19.8)	P	G (83.6)	G (3.64)	OG (16.0)
15	1-Propanol	P	P	OG (7.93)	G (11.5)	OG (83.6)	G (8.09)	G (21.3)
16	1-Butanol	P	-	G (19.8)	G (17.3)	G (83.6)	G (18.2)	G (32.0)
17	1-Pentanol	P	G (92.5)	OG (10.6)	G (11.0)	G (83.6)	G (10.4)	G (5.82)
18	Cyclohexanol	P	-	G (26.4)	G (69.0)	G (83.6)	OG (72.8)	P
19	1-Octanol	P	-	G(39.6)	G (23.0)	OG (83.6)	G (14.6)	OG (32.0)
20	1-Dodecanol	P	-	G(79.3)	P	OG (83.6)	G (58.2)	OG (64.0)
21	Acetone	P	P	G (6.34)	G (7.67)	OG (27.9)	OG (9.71)	G (8.01)
22	Methylethylketone	P	G (30.8)	G (7.93)	G (23.0)	OG (83.6)	OG (11.2)	G (10.7)
23	Dimethoxyethane	P	G (92.5)	G (19.8)	G (13.8)	P	G (58.2)	G (12.8)
24	Triethylamine	P	P	G (7.93)	G (11.5)	OG (83.6)	G (7.28)	G (4.91)
25	DMSO	OG (24.6)	-	OG (13,2)	OG (8.63)	OG (41.8)	OG (4.85)	P
26	Dioxane	P	G (92.5)	OG (15.9)	P	OG (83.6)	G (6.62)	G (5.34)
27	Toluene	P	P	G (22.7)	P	P	G (12.1)	P
28	Pyridine	P	G (92.5)	G (79.3)	S	S	G (72.8)	G (16.0)

[a] The values in parentheses are CCG. The molecular weight of the halogens varies widely, in order to be able to compare the gelling ability based on the CCG the values are expressed in mM. Inverted tube test code G: transparent gel, OG: opaque gel, I: Insoluble, S: soluble; P: soluble after heating but precipitate upon cooling.

View Article Online
DOI: 10.1039/D0NJ01440K

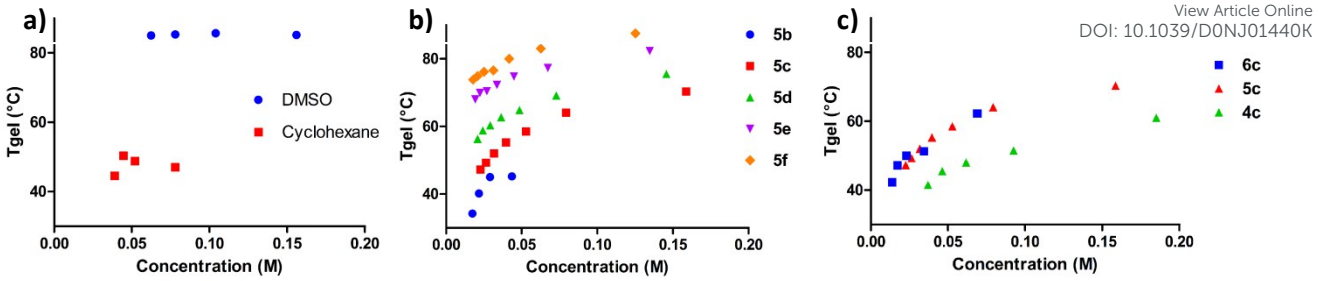

Fig. 3 Thermal stability (T_{gel}) vs. concentration plots measured using the inverted tube method. a) non-halogenated gelator **2f** in DMSO and cyclohexane. b) Effect of the alkyl chain length for the brominated gelators **5b-f** in ethanol c) Halogen effect (Cl, Br and I) for the laurylamide derived gelators in ethanol.

The rest, with alkyl chains from 12 to 18 carbon atoms, turned out to be highly efficient gelators for a wide spectrum of solvents (Table S3). The only solvents that could not be gelled were water, acetic acid and methanol. Most of the gels were transparent, evidencing a good balance of solvophobicity and solvophilicity. In some solvents, like acetonitrile (ACN), compounds **5c-e** can be considered supergelators, as they require a very low concentration to gel with CCG around 0.29-0.67 mM. Comparing with the reported dibrominated gelator **1**, which in the same solvent required a concentration of 0.05M, it can be concluded that the presence of the amides (hydrogen bond donor and acceptor) enhances about 170 manifold the gelling ability in ACN. In this case there is not a defined optimal chain length; gelators **5c-f** have all a very good gelling ability in different solvents and have similar CCG values. This result suggests that the bromine atom has a strong positive effect on the formation of the SAFIN and an alkyl chain of more than 12 carbon atoms does not influence the gelling ability as observed for the chlorinated gelators. Finally, changing bromine for iodine caused a decrease in the gelling ability, reflected in a smaller number of gelled solvents and, in general, higher CCG (Table 1 and Table S4). Gelators **6c** and **6d** had the best gelling scope, being compound **6d,** with alkyl chain of 14 carbon atoms, the best iodinated gelator. Comparing the gelling ability of gelators bearing the same alkyl chain (Table 1 and S5-6) it is also notable that the gelling ability for the first three halogens improves in the order F < Cl < Br, but this tendency is lost with iodine that has a lower gelling ability than the brominated analogues, with some exceptions. For example, in non-polar solvents such as hydrocarbons the gelling ability of laurylamides gelators follows the progressive tendency expected for halogens F < Cl < Br < I. This can be attributed to the fact that the presence of the highly polarizable iodine atoms considerable increases the solubility, especially in polar solvents, and a higher concentration is needed to build up the SAFIN.

Thermal stability

All gels obtained were thermo-reversible, thus, they turned into a fluid solution after heating and gelled again after cooling to room temperature. Determination of the T_{gel} and its dependence with concentration was performed in order to determine the halogen and alkyl chain length effect on the thermal stability of the gels. T_{gel} were measured using the inverted tube test on selected solvents. The T_{gel} of the non-halogenated and fluorinated gelators showed little dependence with concentration, reaching a constant maximum T_{gel} near the CCG (Fig. 3a). The DMSO gel of gelator **2f** showed the higher thermal stability with a constant T_{gel} of 85 °C in the whole concentration range.

Gelators **4**, **5** and **6** showed the typical behaviour of molecular gels (Fig. 3b,c see ESI† Fig. S1-5). As the concentration of gelator increased, the T_{gel} also increased with convergence to a plateau region were the T_{gel} had little dependence with the concentration. From the study it is clear that, for a given halogen and solvent, as the alkyl chain length increases (from 10 to 18 carbon atoms) the thermal stability also increases in a systematic way (Fig. 3b, Fig. S3 and S4). On the other hand, the alkyl chain length has, generally, a higher effect on the CCGs in non-polar solvents like hydrocarbons and CCl_4 (Tables S2-S5). The halogen effect on the thermal stability was not as important (Fig 3c and Fig. S5). Comparison of the thermal stability of chlorinated, brominated and iodinated gelators with the same alkyl chain showed that the chlorinated gelators are always the less thermostable followed, respectively, by the brominated and iodinated gelators. In particular the brominated and iodinated gelators with laurylamides have very similar thermal stability (Fig. 3c).

Dynamic Rheology

Rheology analyses were performed to assess the viscoelastic nature and the mechanical strength of the gels. The mechanic spectra, storage (G´) and loss (G´´) moduli vs. frequency, of different samples were measured. The effect of the halogen on the mechanic spectra of gels in ethanol is shown in Fig. 4a. All organogels showed the typical viscoelastic behavior of supramolecular gels: G´ was greater than G´´ in at least 1 order of magnitude, with small frequency dependence.[48] Comparing the mechanical spectra of the halogenated gelators with the same alkyl chain a remarkable elastic strength difference can only be attributed to the halogen substituents (Fig. 4a). Gelator **5c** (bearing bromine) rendered the stiffer organogel followed by the iodinated and the chlorinated gelators respectively. This result is in line with the gelling ability observed in the CCG, gelling scope and thermal stability. On the other hand, the alkyl chain also has an important effect.

View Article Online
DOI: 10.1039/D0NJ01440K

Gelator **5b** (with the shorter alkyl chain) turned out to be the weakest gel with the lowest modulus values in the frequency range of 0.1-10 Hz (Fig. S6). From 10 Hz frequency dependence of the elastic modulus arose and the fluid-like behavior started to dominate at 18 Hz where a cross of both moduli evidenced the predominance of viscous over elastic behavior. As the alkyl chain length increased, both modulus (G´ and G´´) as well as the viscoelasticity linear range also increased accounting for a higher mechanical stability. Gelator **5f**, with stearylamides, was the most stable with the highest G´ and G´´ moduli with slight dependence. The storage modulus (at 1 Hz) was evaluated as a function of temperature in order to study the temperature effect on the mechanical strength of the organogels with different alkyl chain length (Fig. 4b) and halogens (Fig. 4c). The thermal stability and T_{gel} values were then analysed based on the G´ value decrease, which is indicative of the gradual transformation from gel to sol. For all gels it could be observed that the temperature at which the drop of the storage modulus occurred coincided with the T_{gel} measured with the inverted tube method at the same concentration (Fig. 3). For a given halogen, for example bromine, as the alkyl chain length increased both thermal stability and mechanical strength increased as reflected by higher T_{gel} and G´ modulus (Fig. 4b). In addition, the halogen effect can be revealed comparing gelators with the same alkyl chain (Fig. 4c). Iodinated gelators rendered the more thermostable gels with higher T_{gel} and a slower decreasing slope. For the 12-carbon alkyl chain derivatives, it can be observed that the chlorinated derivative forms gels with lower T_{gel} and G´ values.

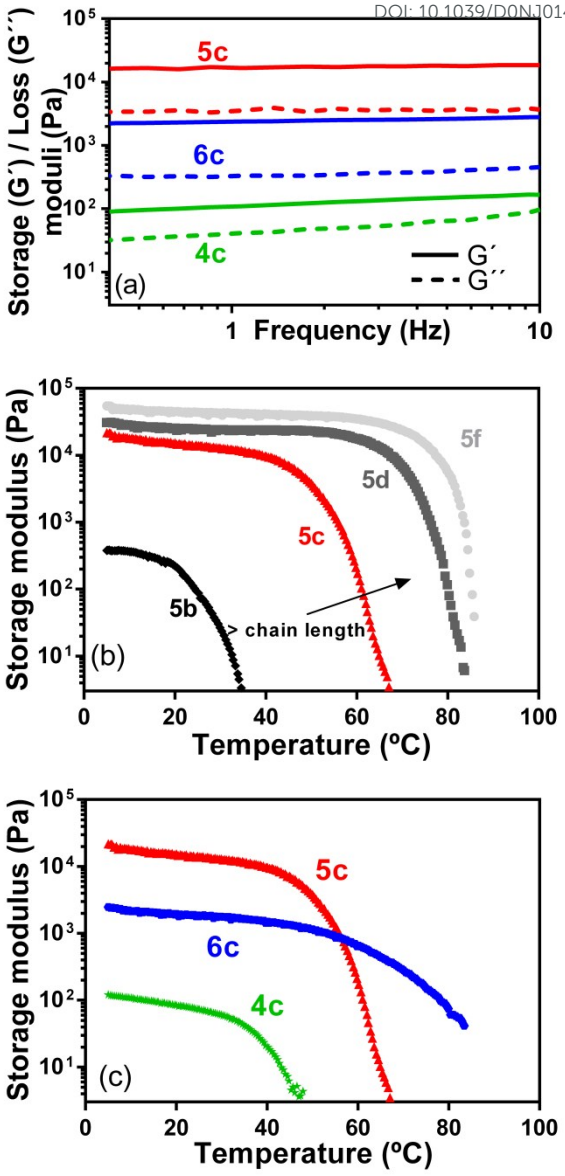

Fig 4. Rheology: a) Storage (G) and loss (G") moduli for chlorinated, brominated and iodinated gelators with the same alkyl chain in ethanol, 25 °C. b) alkyl chain length effect and c) halogen effect on the thermal stability determinded by rheologycal experiment (G` vs T at 1 Hz). Concentration 15 mM.

Morphology

In order to get an insight into the microscopic morphologies of the gels we dried gels from ethanol using the CO_2 supercritical drying process and the aerogels obtained were examined by scanning electron microscopy (SEM). We chose this drying method because supercritical conditions better preserve the microscopic structure of supramolecular gels from collapsing as it is usually observed using the typical vacuum drying process.[56,57] In all cases a crossed-link fibrillar network was observed with fibers several micrometers length (Fig. 5). The diameter of the fibers was dependent on the alkyl chain length but independent on the halogen. Among the brominated gelators the thinnest fiber was observed for **5b** bearing the shorter alkyl chain (caprilamides) showing also the less entangled fibrillar network (Fig. 5a). As the alkyl chain increased, the diameters also increased from 20 nm for **5c**, to 25 nm for **5d** and 30 nm for **5f** (Fig. 5) with the longest alkyl chain (stearylamides). The same trend was observed with the other halogens (Fig. S7-S10). Comparing the images among gelators with the same alkyl length, the brominated gelators showed a more entangled SAFIN, in concordance with their better gelling ability and higher stability.

Organogel SAFIN as template

The SAFINs of molecular gels can be, sometimes, successfully used as template for the preparation of nanostructured inorganic materials. For example SiO_2 and other inorganic oxides nanomaterials (usually nanotubes) can be synthetized following an *in situ* polymerization process from TEOS or other metal alkoxides respectively.[44,58] This is interesting not only for the potential applications of the inorganic nanostructured materials, but also because the *in situ* template polymerization gives information about the morphology of the SAFIN in gel phase. We tested the *in situ* polymerization of TEOS and $Ti(OiPr)_4$ using as template organogels of compound **5f** in ethanol. In both cases hollow nanotubes were obtained with an internal diameter of around 30 nm (Fig. 6). This is in agreement with the dimensions of the fibers observed in the aerogels, so we can conclude that the supercritical drying conserved the SAFIN structure present in the organogel.

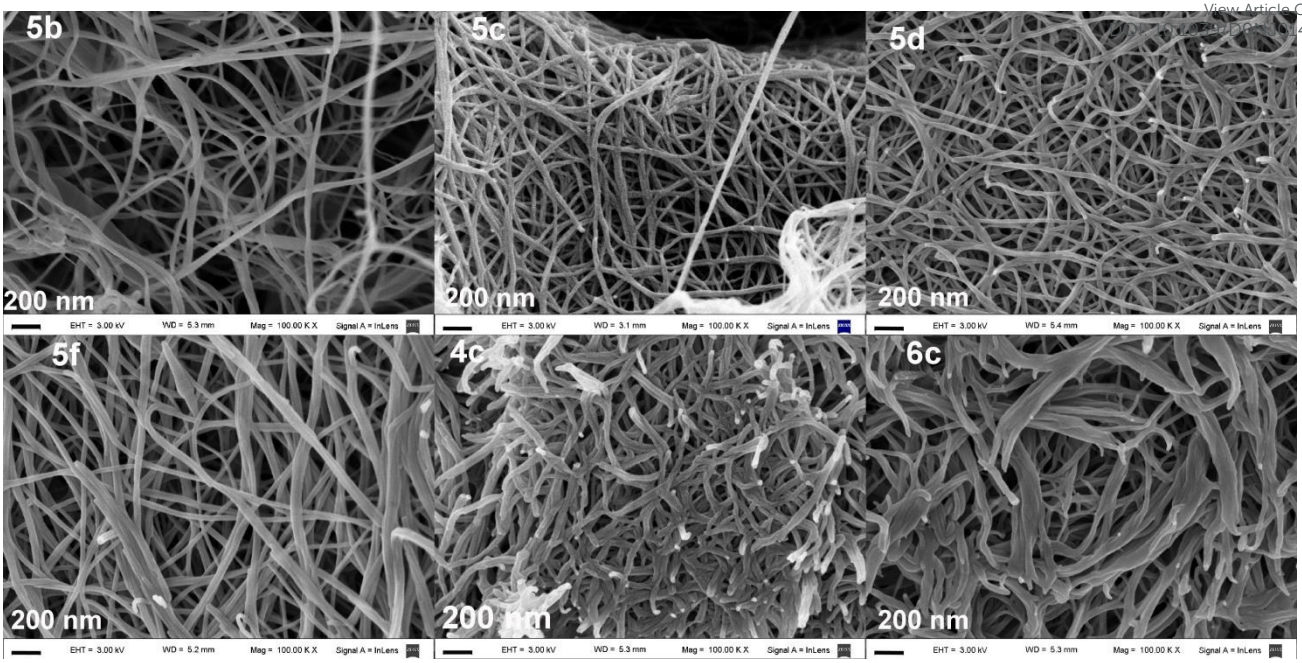

Fig 5. Comparative Aerogel images (SEM) obtained from gels in ethanol of brominated gelators bearing different alkyl chain length: **5b** (caprilamides), **5c** (laurylamides), **5d** (myristoylamides), **5f** (stearylamides) and gelators bearing laurylamides with different halogens: **4c** (chlorinated), **5c** (brominated) and **6c** (iodinated) gelators. Mag. = 100.00 K X. Scale bar 200 nm.

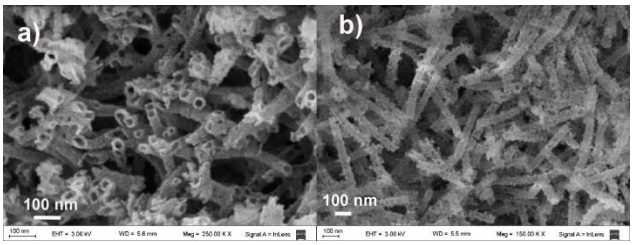

Fig. 6 SEM images of the nanotubes prepared following an *in situ* polymerization process using an organogel of **5f** in ethanol as template: a) TiO_2 and b) SiO_2. Internal diameters 30 nm.

This also indicates that the negatively charged silicates and titanates species formed during the process were able to interact with the SAFIN allowing the polymerization to take place at the surface of the fibers that could act as template.

Investigation on the Self-assembly mode

Variable concentration ^{1}H NMR spectroscopy. To get an insight into the supramolecular forces involved in the self-assembly we studied the ^{1}H NMR variation with concentration (Fig. S11). As the brominated derivatives resulted to be the best gelators we carried out the study above and below the CCG of gelator **5f** in $CDCl_3$ (0.71 %wt/v). As the concentration increased from 0.5 to 1 %wt/v, the sign of the aromatic protons showed a gradual upfield shift from 7.65 to 7.59 ppm, this shielding effect is indicative of intermolecular π-π interactions. Furthermore, the NH signal showed a downfield shift from 8.16 to 8.28 ppm. Typically the presence of hydrogen bond interactions induces charge transfer and polarization leading to a de-shielding effect of the proton involved. This demonstrates that as the concentration increased, the molecular aggregation also increased based on π-π stacking and hydrogen bond interactions.

Small angle X-ray scattering (SAXS). The structures of the self-assembled systems present in the gels were also studied by SAXS. This technique can be used to estimate on average the shape and size of objects in the range on a few nm of size. Since molecular gels are diluted systems it is not always possible to obtain a useful dispersion curve. In the particular case of bromine and iodine, the high density of these atoms provided a high electronic density contrast compared to solvent, that allow to obtain a good dispersion curve for the used concentrations. We analyzed gels of the brominated and iodinated gelators in different solvents and only obtained useful data for gels of **5c** in ethanol and **6c** in 1-pentanol. The dispersion curve as a function of the modulus of *q* obtained for **5c** and **6c** are shown in Fig. 7. In order to give an estimation of the shape and size of the nano-objects a simple model of a core-shell cylinder[59] was used that is implemented in the SASView code.[52‡]

Different core/shell relative densities were fixed during the fitting routine and, in both systems, the SAXS data modeling is compatible with a cylindrical object with a low density core, and a thin high density shell (Fig. 7a and 7b). Therefore, from these results it can be deduced that the halogen atoms are located in the shell of the cylinder. The short length of the cylinders (around 5.5 Å) indicated that the system may be better described as a set of stacked discs shaped objects. Thus, a stacked discs cylinder model[59] implemented in the SASView code was used in order to test this idea. This model considers repetitive stacking of a core and a separation layer of uniform

View Article Online
DOI: 10.1039/D0NJ01440K

densities with disc shaped objects. For the core disc density we considered an intermediate density between the densities obtained in the core-shell cylinder model. The complete parameters of the fitting routines for are shown in the ESI†. A good fitting agreement obtained with both cylindrical models encouraged us to describe the systems as being formed by the stacking of core-shell discs (Fig. 7c) with dimensions for the core diameter of around 40.0 and 44.2 Å for the brominated and iodinated gelators with shells 2.0 Å thick and an overall diameter of 44.0 and 48.2 Å. These dimensions are in accordance with the length of an elongated molecule of the gelators. Fixing the solvent density at 0.77, the relative densities or the core and shell were estimated to be ρ_{shell}/ρ_{core} = 1.55 for the brominated gelator **5c** and ρ_{shell}/ρ_{core} = 2.91 for the iodinated gelator (Fig. 7).

To prove that the SAXS dispersion observed were generated by the SAFIN, variable temperature SAXS experiments were performed in both gels between 21-70 °C (Fig. S13). As the temperature increased, the SAXS dispersion curves gradually loosed the form factor that completely disappeared after reaching the T_{gel} accounting for the molecular disassembly of the SAFIN (Fig. S13, ESI†). Based on these results we propose the self-assembly mode depicted in Fig. 7c where the discs are formed by gelator molecules with their non-polar alkyl chain pointing to the core and the halogen atoms at the exterior rim of the discs, stacked each other through hydrogen bond and π-π interactions. The cylinders, then, would be able to interact with other cylinders by halogen-halogen contacts to generate the cross-linked SAFIN that leads to the organogel.

X-Ray Diffraction Study. Elucidating in detail the self-assembly mode involved in gelation at the molecular level is difficult. In some cases gelators have a similar mode of packing in crystals and gel state and this can be used to gain information on the assembly by comparing the powder X ray diffraction (PXRD) patterns of crystals and xerogels.[36] If they match, the crystal structure can be used to understand the molecular assembly in the gel. However we could not use this strategy; all attempts to obtain a single crystal of any of the gelators failed, either because of their high gelling capacity (it was not possible to find a crystallization solvent) or the crystals obtained were too small or did not diffracted at all. Nevertheless, in order to get an insight on the molecular interactions and halogen contacts that may be involved in the microstructure of the gels of this family of gelators, we have synthetized an analogue of gelator **4c** bearing only one alkylamide moiety (compound **7**, Fig. 8). Compound **7** could not gel any solvent but, did give place to crystals easily obtained from acetone and thus, its structure was solved using Single Crystal X-ray Diffraction studies (for details see ESI†). The crystal packing of compound **7** is sustained by N–H···O=C H-bonds between the amide moieties with a distance d_{O1H1} = 2.11 Å, resulting in an infinite chain along crystallographic axis *c* (Fig. 7, ESI†). In this case a halogen contact between Cl1 substituents of consecutive molecules with a d_{Cl1Cl1} = 3.516 Å and $\angle_{C3Cl1Cl1}$ = 150.20° (Fig. 8) is observed; based on this geometry, it can be classified as Type I halogen contact. This interaction involves two molecules and is extended alternatively along the structure and intercalated with the N–H···O=C H-bond chains.

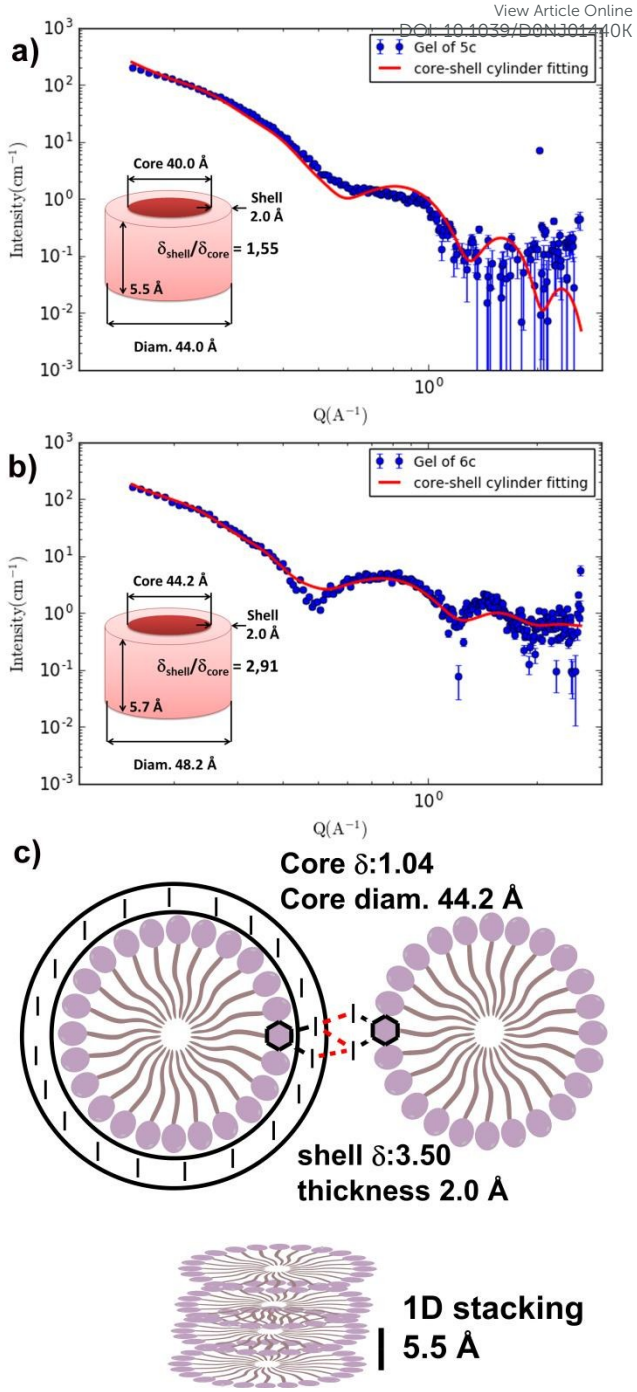

Fig 7. SAXS for a gels of compounds **5c** in ethanol (a) and **6c** in 1-pentanol (b) and the fittings obtained with the core-shell cylinder model. Inset figures show the dimensions and relative densities obtained from the fitting in each case. Based on these results a self-assembly model with the halogens atoms located at the surface of the fiber can be proposed (c). For the stacked disc cylinder fitting see ESI†.

View Article Online
DOI: 10.1039/D0NJ01440K

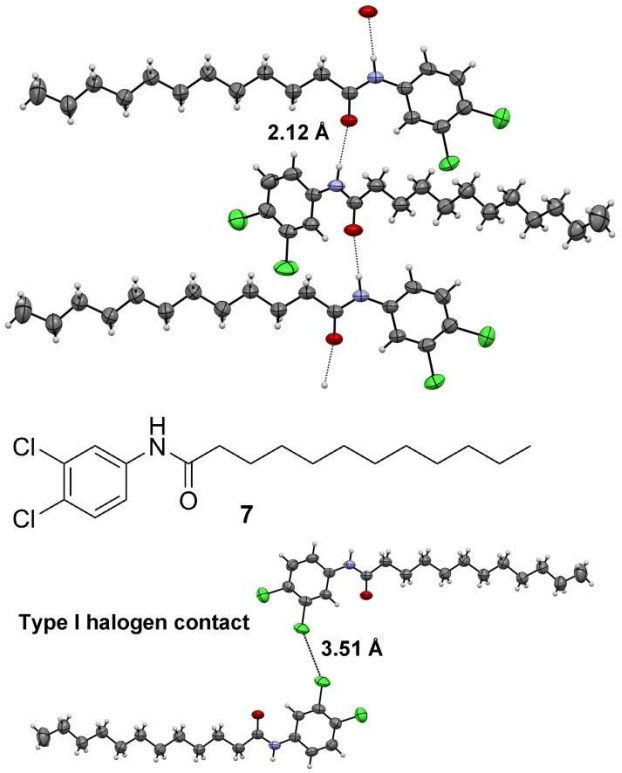

Fig 8. Crystal structure of compound **7** determined by single crystal XRD using ORTEP diagram with ellipsoids at 50% displaced along crystallographic bc plane. Colour code: H, light grey; C, grey; N, light blue; O, red; Cl, green. Hydrogen bonds and halogen contacts are represented with dotted lines.

The other Chlorine atom experiments non-conventional H-bonds involving the hydrogens of the aromatic ring and one of the methylenes of the alkyl chains. In brief, for compound **7** with only one long alkylamide, type I chlorine contacts are stabilizing the crystal structure. Single crystals of compound **5a** were also easily obtained from acetone (see ESI†). The crystal packing is also sustained by N–H···O=C H-bonds between amide moieties with a distance d_{O1H1} = 2.012 Å (see ESI†). The resulting arrangement is given by the interaction between the carbonyl of one branch and the NH of the adjacent molecule, and *vice versa*. The result is an infinite chain extended along the crystallographic axis *c*. As consequence of this main interaction other short contacts are also developed such as non-conventional C-H···O hydrogen bond between the aromatic ring and a carbonyl. Based on the crystal structure of the reported gelator **1**, it was expected the development of halogen bonds concerning the bromide substituents. In **5a** bromine atoms of one molecule face the end of the amide branches of another one and consequently, no short X···X contacts are possible. Based on these crystal structures a Hirshfeld surface analysis has been performed for compounds **7**, **5a** and the reported gelator **1**, by using Crystal Explorer17 program.[60] The Hirshfeld surface analysis is a valuable method for the analysis of intermolecular contacts that offers a whole-of-the-molecule approach.[61] The 2D fingerprint plots of the

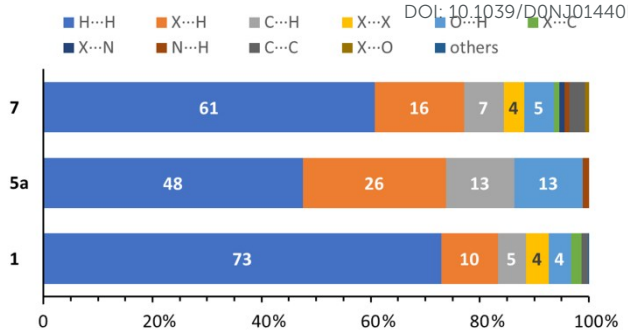

Fig. 9 Relative contributions of intermolecular contacts to the Hirshfeld surface. Compound **7** (top), compound **5a** (middle) and gelator **1** (bottom). Van der Waals (H···H), hydrogen bond (O···H) and halogen contacts (X···X).

crystal structure of compounds **5a**, **7** and **1** were performed (see ESI†) in order to have a tool to compare the predominant short contacts in each system determining the relative contribution of intermolecular contacts to the Hirshfeld surface area (Fig. 9). Based on the reported crystal structure of compound **1**,[40] a very poor gelator,[39] the preponderant interactions are Van der Waals forces (H···H) associated with the alkyl chains followed by X···H; C···H and X···X contacts respectively. Compound **5a** with two shorter alkyl chains of 7 C atoms, has a smaller Van der Waals surface contact with a higher hydrogen bond surface related with the presence of two amide functions and, as expected, X···X contacts are absent. For compound **7** with only one amide and a 12 C alkyl chain, the Van der Waals contacts have a very important contribution. So, for long-chain compounds **1** and **7**, the packing of the aliphatic chains seems to be the main driving force for the crystal structure and in both, halogen contacts are present and also contribute to the stability of the structure. For the shorter chain length compound, the highly and strong hydrogen bond interaction has a predominant contribution to the assembly and the weaker halogen contacts do not contribute significantly to the packing. Thus, the presence of one or two long alkyl chain (at least 12 C) offers a higher non polar surface than two short alkyl chains and would allow the formation of halogen contacts. This analysis extrapolated to the gel SAFIN highlights the importance of the long alkyl chain length, in line with the self-assembly proposed based on SAXS experiments. As compound **7** cannot gel any solvent these results suggest that the two amide functions are essential to provide a good intermolecular hydrogen bond interaction, together with a high non polar surface given by long alkyl chains of at least 12 C atoms.

Conclusions

We have designed and synthetized a new family of efficient and versatile low molecular weight gelators based on N,N'-(4,5-dihalo-1,2-phenylene)dialkylamides bearing fluorine, chlorine, bromine and iodine and different alkyl chain lengths. The pronounced effect of the vicinal di-halogen moiety was

studied and evidenced by their gelling ability, thermal stability and mechanical properties. Considering the general gelling ability, reflected in the critical concentration for gelation (CCG) and the variety of solvents gelled, brominated gelators are the most versatile and powerful with an outstanding ability to gel 31 of the 34 solvents tested with exception of water, acetic acid and methanol. In some solvents like acetonitrile they have a supergelling ability with minimal concentration for gelation as low as 0.29 mM (0.02 %wt/v). These brominated gels show a higher crossed linked SAFIN that is directly related to their higher stability. Specifically in hydrocarbons the gelling ability increased from fluorine to iodine following the halogen bond donor ability trend (F<Cl<Br<I). In the rest of the solvents (polar liquids) bromine has the optimal balance of solubility (solvophobic/solvophilic effect) and self-assembly but with iodine this balanced is broken in more polar solvents probably due to its higher polarizability. Variable concentration ^{1}H NMR experiment indicates that hydrogen bond and π-π stacking are the driving forces for the 1D self-assembly. SAXS experiments allowed us to propose a mode of self-assembly for gels in ethanol based on a stacked discs cylinder where the halogen atoms are located at the surface of the cylindrical fibers interacting with the solvent and involved in the cross-linking through halogen-halogen contacts that leads to the SAFIN. These results indicate that the self-assembled fibrillar network is directly involved with the halogen bond donor ability. The key interaction to form the self-assembled gels were found to be the hydrogen bond, Van der Waals interactions and π-π stacking, directing the 1D assembly, while halogens are involved in the cross-linking of the fibrillar network through halogen contacts. As it is usually observed in LMWGs, the length of the alkyl chain is also highly important in order to have the gelling ability, providing a high non-polar surface.

Thus, this work provides a novel strategy to design new π-gelators or to improve and tune the efficiency of known low molecular weight organogelators by introducing two vicinal halogen substituents into an aromatic ring. Furthermore, an ethanolic gel was successfully used as template to prepare silica and titania nanotubes, an indication of good interaction between the negatively charged silicates and titanates species formed during the hydrolytic polymerization with the halogens at the surface of the fibers, allowing a template process. Hence, such organogels are promising materials for future research and development.

Conflicts of interest

There are no conflicts to declare.

Acknowledgements

We acknowledge Universidad de Buenos Aires (grant 200201500100121BA), CONICET (grant PIP 11220170100736CO) and Agencia Nacional de Promoción Científica y Tecnológica (grant PICT2016-621) for financial support. SAXS experiments at INIFTA were performed thanks to project "Nanopymes" (EuropeAid/132184/D/SUP/AR-Contract31-896).

Notes and references

‡ This work benefited from the use of the SasView application, originally developed under NSF award DMR-0520547. SasView contains code developed with funding from the European Union's Horizon 2020 research and innovation programme under the SINE2020 project, grant agreement No 654000.

1 E. R. Draper and D. J. Adams, *Low-Molecular-Weight Gels: The State of the Art*, Elsevier Inc., 2017, vol. 3.
2 P. Terech and R. G. Weiss, *Chem. Rev.*, 1997, **97**, 3133–3160.
3 R. G. Weiss, *Molecular Gels: Materials with Self-Assembled Fibrillar Networks*, Springer Netherlands, Dordrecht, 2006.
4 C. D. Jones and J. W. Steed, *Chem. Soc. Rev.*, 2016, **45**, 6546–6596.
5 Z. Sun, Q. Huang, T. He, Z. Li, Y. Zhang and L. Yi, *ChemPhysChem*, 2014, **15**, 2421–2430.
6 S. S. Babu, S. Prasanthkumar and A. Ajayaghosh, *Angew. Chemie - Int. Ed.*, 2012, **51**, 1766–1776.
7 S. K. rishn. M. Nalluri, N. Shivarova, A. L. Kanibolotsky, M. Zelzer, S. Gupta, P. W. J. M. Frederix, P. J. Skabara, H. Gleskova and R. V. Ulijn, *Langmuir*, 2014, **30**, 12429–12437.
8 W. P. Singh and R. S. Singh, *Soft Mater.*, 2019, **17**, 93–118.
9 C. Ren, J. Zhang, M. Chen and Z. Yang, *Chem. Soc. Rev.*, 2014, **43**, 7257–7266.
10 W. Fang, Y. Zhang, J. Wu, C. Liu, H. Zhu and T. Tu, *Chem. - An Asian J.*, 2018, **13**, 712–729.
11 J. Mayr, C. Saldías and D. Díaz Díaz, *Release of small bioactive molecules from physical gels*, 2018, vol. 47.
12 C. L. Esposito, P. Kirilov and V. G. Roullin, *J. Control. Release*, 2018, **271**, 1–20.
13 Y. Li, D. J. Young and X. J. Loh, *Mater. Chem. Front.*, 2019, **3**, 1489–1502.
14 B. O. Okesola and D. K. Smith, *Chem. Soc. Rev.*, 2016, **45**, 4226–4251.
15 A. Dey and K. Biradha, *Isr. J. Chem.*, 2019, **59**, 220–232.
16 D. D. Díaz and C. Saldías, *Curr. Org. Chem.*, 2018, **22**, 2223–2228.
17 B. Maiti, A. Abramov, R. Pérez-Ruiz and D. Díaz Díaz, *Acc. Chem. Res.*, 2019, **52**, 1865–1876.
18 J. Guo, X. Yu, Z. Zhang and Y. Li, *J. Colloid Interface Sci.*, 2019, **540**, 134–141.
19 P. R. A. Chivers and D. K. Smith, *Nat. Rev. Mater.*, 2019, **4**, 463–478.
20 R. Weiss, *Gels*, 2018, **4**, 25.
21 J. H. van Esch, *Langmuir*, 2009, **25**, 8392–8394.
22 G. Cavallo, P. Metrangolo, R. Milani, T. Pilati, A. Priimagi, G. Resnati and G. Terraneo, *Chem. Rev.*, 2016, **116**, 2478–2601.
23 R. Tepper and U. S. Schubert, *Angew. Chemie - Int. Ed.*, 2018, **57**, 6004–6016.
24 A. Priimagi, G. Cavallo, P. Metrangolo and G. Resnati, *Acc. Chem. Res.*, 2013, **46**, 2686–2695.

25 M. Saccone and L. Catalano, *J. Phys. Chem. B*, 2019, **123**, 9281–9290.
26 L. Meazza, J. A. Foster, K. Fucke, P. Metrangolo, G. Resnati and J. W. Steed, *Nat. Chem.*, 2013, **5**, 42–47.
27 H. Hu, Y. Qiu, J. Wang, D. Zhao, H. Wang, Q. Wang, Y. Liao, H. Peng and X. Xie, *Macromol. Rapid Commun.*, 2019, **40**, 1–5.
28 Z. X. Liu, Y. Sun, Y. Feng, H. Chen, Y. M. He and Q. H. Fan, *Chem. Commun.*, 2016, **52**, 2269–2272.
29 X. Tong, Y. Qiu, X. Zhao, B. Xiong, R. Liao, H. Peng, Y. Liao and X. Xie, *Soft Matter*, 2019, **15**, 6411–6417.
30 Y. Feng, H. Chen, Z. X. Liu, Y. M. He and Q. H. Fan, *Chem. - A Eur. J.*, 2016, **22**, 4980–4990.
31 Q. Li, R. Li, H. Lan, Y. Lu, Y. Li, S. Xiao and T. Yi, *ChemistrySelect*, 2017, **2**, 5421–5426.
32 Z. Wu, J. Sun, Z. Zhang, H. Yang, P. Xue and R. Lu, *Chem. - A Eur. J.*, 2017, **23**, 1901–1909.
33 A. Pizzi, L. Lascialfari, N. Demitri, A. Bertolani, D. Maiolo, E. Carretti and P. Metrangolo, *CrystEngComm*, 2017, **19**, 1870–1874.
34 D. M. Ryan, S. B. Anderson and B. L. Nilsson, *Soft Matter*, 2010, **6**, 3220–3231.
35 Y. Huang, H. Li, Z. Li, Y. Zhang, W. Cao, L. Wang and S. Liu, *Langmuir*, 2017, **33**, 311–321.
36 A. Prathap, A. Ravi, J. R. Pathan and K. M. Sureshan, *CrystEngComm*, 2019, **21**, 5310–5316.
37 F. F. Awwadi, R. D. Willett, K. A. Peterson and B. Twamley, *Chem. - A Eur. J.*, 2006, **12**, 8952–8960.
38 P. Metrangolo and G. Resnati, *IUCrJ*, 2014, **1**, 5–7.
39 G. Clavier, M. Mistry, F. Fages and J. L. Pozzo, *Tetrahedron Lett.*, 1999, **40**, 9021–9024.
40 A. Fonrouge, F. Cecchi, P. Alborés, R. Baggio and F. D. Cukiernik, *Acta Crystallogr. Sect. C Cryst. Struct. Commun.*, 2013, **69**, 204–208.
41 I. Muñoz Resta, V. Manzano, F. Cecchi, C. Spagnuolo, F. Cukiernik and P. Di Chenna, *Gels*, 2016, **2**, 7.
42 E. L. Bonifazi, V. C. Edelsztein, G. O. Menéndez, C. Samaniego López, C. C. Spagnuolo and P. H. Di Chenna, *ACS Appl. Mater. Interfaces*, , DOI:10.1021/am5010656.
43 M. E. Cano, P. H. Di Chenna, D. Lesur, A. Wolosiuk, J. Kovensky and M. L. Uhrig, *New J. Chem.*, 2017, **41**, 14754–14765.
44 V. C. Edelsztein, A. S. Mac Cormack, M. Ciarlantini and P. H. Di Chenna, *Beilstein J. Org. Chem.*, 2013, **9**, 1826–36.
45 US 6726915 B2, 2004.
46 F. D. Cukiernik, A. Zelcer, M. T. Garland and R. Baggio, *Acta Crystallogr. Sect. C Cryst. Struct. Commun.*, 2008, **64**, 604–608.
47 G. W. H. Cheeseman, *J. Chem. Soc.*, 1962, 1170–1176.
48 A. Dawn and H. Kumari, *Chem. - A Eur. J.*, , DOI:10.1002/chem.201703374.
49 R. H. Blessing, *Acta Crystallogr. Sect. A Found. Crystallogr.*, 1995, **51**, 33–38.
50 L. J. Bourhis, O. V. Dolomanov, R. J. Gildea, J. A. K. Howard and H. Puschmann, *Acta Crystallogr. Sect. A Found. Adv.*, 2015, **71**, 59–75.
51 G. M. Sheldrick, *Acta Crystallogr. Sect. A Found. Adv.*, 2015, **71**, 3–8.
52 SasView application, http://www.sasview.org/.
53 E. Önal, F. Dumoulin and C. Hirel, *J. Porphyr. Phthalocyanines*, 2009, **13**, 702–711.
54 X. De Hatten, D. Asil, R. H. Friend and J. R. Nitschke, *J. Am. Chem. Soc.*, 2012, **134**, 19170–19178.
55 P. Zimcik, M. Miletin, H. Radilova, V. Novakova, K. Kopecky, J. Svec and E. Rudolf, *Photochem. Photobiol.*, 2010, **86**, 168–175.
56 B. Jamart-Grégoire, S. Son, F. Allix, V. Felix, D. Barth, Y. Jannot, G. Pickaert and A. Degiovanni, *RSC Adv.*, 2016, **6**, 102198–102205.
57 F. Placin, J.-P. Desvergne and F. Cansell, *J. Mater. Chem.*, 2000, **10**, 2147–2149.
58 M. Llusar, *Chem. Mater.*, 2008, **20**, 782–820.
59 S. R. Kline, *J. Appl. Crystallogr.*, 2006, **39**, 895–900.
60 U. of W. A. M. J. Turner, J. J. McKinnon, S. K. Wolff, D. J. Grimwood, P. R. Spackman, D. Jayatilaka and M. A. Spackman, CrystalExplorer17, 2017.
61 M. A. Spackman and D. Jayatilaka, *CrystEngComm*, 2009, **11**, 19–32.

View Article Online
DOI: 10.1039/D0NJ01440K

Vicinal di-halo substituents have a determinant effect on the supramolecular self-assembly and properties of aromatic physical gelators with application as soft templates